Full-Field Strains in an Intact and Torn Rotator Cuff Animal Model Using Magnetic Resonance Imaging

C.N. Villacís Núñez[1a], U. Scheven[1], A. Bedi[4], and E.M. Arruda[2,3]

Departments of [1]Mechanical Engineering, [2]Biomedical Engineering, and [3]Macromolecular Science and Engineering, University of Michigan, USA, 2101 Bonisteel Blvd, Ann Arbor, MI 48109, [4]NorthShore Orthopedic and Spine Institute, USA, 680 N Lake Shore Dr Ste 924 & 925, Chicago, IL 60611

[a]carlanvn@umich.edu

Abstract. Material heterogeneity and the natural curvature of the enthesis complicates the biomechanical characterization of the risk of progression and propagation of partial-thickness rotator cuff tendon tears, using traditional surface strain measurement techniques. In this study, we employ a novel magnetic resonance imaging (MRI)-based method to overcome these challenges. Volumetric deformation of intact and partially torn ovine rotator cuff tendons is obtained. Full-field Lagrangian and maximum principal strain maps are acquired at physiologically relevant loads. The data reveals that strain gradients/concentrations appear close to bone prominent features and regions close to the tear, which suggest changes in load-bearing mechanisms due to small partial-thickness tears. This provides insight into tear propagation mechanisms, which may allow for the development of strain-based markers that indicate type-specific risk of tear progression and propagation.

Introduction

Rotator cuff tendon tears are a leading cause of morbidity and economic loss secondary to musculoskeletal injury, affecting 23% of the general population [1]. These tears most commonly occur at the greater tuberosity tendon-to-bone attachment (enthesis) [2]. High-grade partial-thickness injuries that involve more than 50% of the tendon's footprint (type III tears) and full-thickness tears are often repaired surgically. While nonoperative treatment is an option, the risk of propagation is poorly understood for various tear types and locations (type I: <25% thickness, type II: <50% thickness), relying on anecdotal evidence to arrive at a surgical decision. Surface strain measurement methods have been used to mechanically characterize and predict tear propagation [3]. However, the heterogeneous nature of the supraspinatus tendon and its curved insertion to the humeral head prevent the identification of intratendinous features or strain concentrations that may arise in the articular surface – which is not visible at the neutral position – in the presence of a tear. The aim of the present work is to employ our recently developed full-field strain characterization technique to compare rotator cuff tendons in their intact and partial-thickness tear state, using an animal model of the supraspinatus tendon (ovine infraspinatus tendon). The potential of tear propagation and progression are analyzed from a biomechanical perspective.

Methods

The infraspinatus tendon was isolated from six fresh ovine shoulders, preserving the humeral attachment. Samples were mounted at approximately 0 degrees abduction and rotation into custom-designed 3D printed fixtures and inserted into a magnetic resonance imaging (MRI)-compatible apparatus (Fig. 1-a). Cyclic uniaxial tension in the longitudinal direction occurred in synchrony with a displacement encoding protocol, termed alternating pulsed gradient stimulated echo imaging (APGSTEi) [4], inside a 7T small animal MRI coil. This protocol has been described and tested in intact samples before, and captures through thickness phase variation between deformed and undeformed configurations [4-6]. We employed an isotropic surrogate model of the tendon (silicone) to validate this method in torn configurations (data not shown).

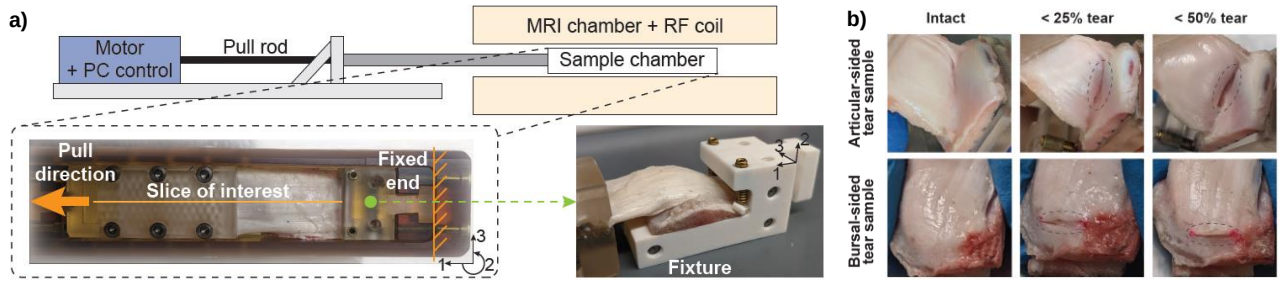

Fig 1. Experimental setup, a) MRI-compatible device and fixture with ovine infraspinatus tendon, b) Consecutive tears in the articular and bursal surfaces.

Full-field Lagrange and principal strains were calculated from these phase variation maps with custom-developed MATLAB codes. The tendons were divided into two groups: articular-sided (3 tendons) and

bursal-sided (3 tendons) tears. Three clinically relevant conditions were tested in each sample, (i) intact tendon, followed by (ii) < 25% footprint detachment (resembling type I tear), followed by (iii) < 50% footprint detachment (resembling type II tear), for both the articular-sided and bursal-sided groups (Fig. 1-b). Two physiologically relevant target loads were analyzed for each condition, 90 N and 180 N, for a total of six experiments per tendon. The 180 N load represented the maximum force during abduction and external rotation in a human shoulder [3].

Results

Our preliminary Lagrangian strain maps showed the capability of our method to characterize small tears in the non-visible surface of a rotator cuff tendon animal model in a repeatable fashion. These strain maps presented a complex three-dimensional distribution with pronounced strain gradients in articular areas close to bone prominent features in both low-load and high-load regimes, for both tear sides. The mid-substance of the tendon deformed to a higher degree in the direction of loading as compared to the region close to the enthesis. The high load configuration showed overall increase in strain values for all tendons, regardless of the tear side, as expected. In the low load regime and some high load cases, maximum principal strain concentration areas close to the attachment were accentuated and rechanneled into regions close to the tear for both the articular-sided and bursal-sided tears (Fig. 2-a). During high loads, these strain concentrated areas were also observed in the mid-substance of the tendon with increasing tear size (Fig. 2-b).

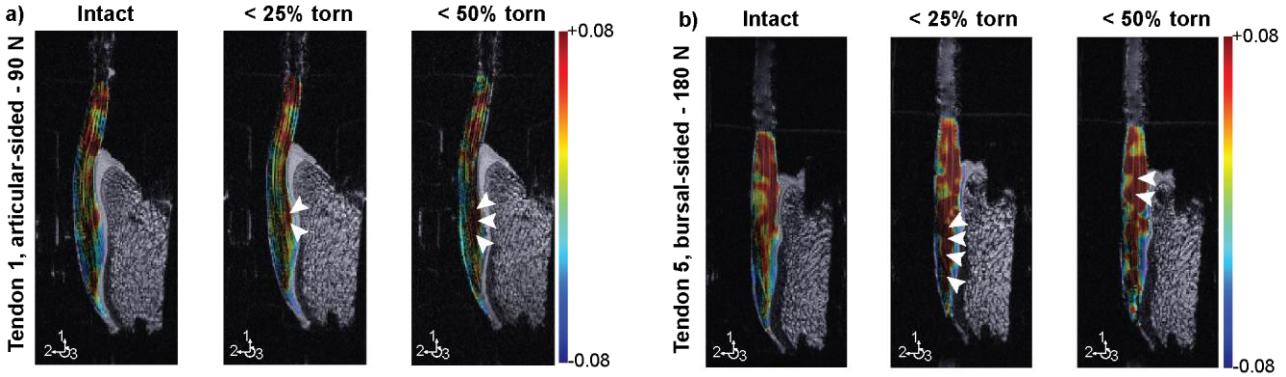

Fig. 2. a) Tendon with articular-sided and b) bursal-sided tear, with redirection of strains to areas close to the tear or the mid-substance of the tendon shown by white arrowheads.

Conclusion

With our novel MRI-based strain measurement technique, we were able to identify differences in the Lagrangian strain maps between the intact and progressively torn conditions, with strain redistribution to regions close to the tear at low loads. Our method enabled the visualization of potential predominance of mode I failure onset, and the plausibility that a relatively small partial-thickness tear could significantly modify how load is distributed within the tendon in proximity to the tear. Importantly, our maps show load redirection that could potentially deform the biomechanical environment and concentrate strains in non-naturally load-bearing sites, which may lead to tear propagation. Consistent larger deformation in bursal-sided tear specimens as compared to articular-sided tear samples might indicate that contact with cartilage is a natural support mechanism, as has been suggested by some previous studies [3]. Future work includes testing samples loaded in the supraphysiological regime, and various full-thickness tear patterns, using our MRI technique that shows the potential of identifying tears at high risk of propagation and defining a threshold for surgical repair with high fidelity.

References

[1] A. Yamamoto et al. *Prevalence and risk factors of a rotator cuff tear in the general population*. J Shoulder Elbow Sur. Vol 19 (2010), p. 116-120.
[2] K.H. Mike et al. *Location and initiation of degenerative rotator cuff tears: an analysis of three hundred and sixty shoulders*. J Bone Joint Surg. Vol. 92 (2010) p 1088.
[3] N. Andarawis-Puri et al. *Rotator cuff tendon strain correlates with tear propagation*. J. Biomech. Vol 42 (2009) p 158-163.
[4] U.M. Scheven et al. *Robust high resolution strain imaging by alternating pulsed field gradient stimulated echo imaging (APGSTEi) at 7 Tesla*. J. Magn. Reson. Vol. 310 (2020) p 106620.
[5] C.M. Luetkemeyer et al. *Constitutive modeling of the anterior cruciate ligament bundles and patellar tendon with full-field methods*. J Mech Phys Solids. Vol. 156 (2021) p 104577.
[6] J.B. Estrada et al. *MR-u: material characterization using 3D displacement-encoded magnetic resonance and the virtual fields method*. Exp. Mech. Vol. 60 (2020) p 907-924.